European Journal of Radiology 106 (2018) 150–159

Contents lists available at ScienceDirect

European Journal of Radiology

journal homepage: www.elsevier.com/locate/ejrad

Research article

# Imaging Phenotypes in Women at High Risk for Breast Cancer on Mammography, Ultrasound, and Magnetic Resonance Imaging Using the Fifth Edition of the Breast Imaging Reporting and Data System

Maria Adele Marino[a,b], Christopher C. Riedl[c], Maria Bernathova[a], Clemens Bernhart[a], Pascal A.T Baltzer[a], Thomas H. Helbich[a,*], Katja Pinker[a,d]

[a] Department of Biomedical Imaging and Image-guided Therapy, Division of Molecular and Gender Imaging, Medical University of Vienna, Waehringer Guertel 18-20, 1090, Vienna, Austria
[b] Department of Biomedical Sciences and Morphologic and Functional Imaging, University of Messina, Via Consolare Valeria 1, 98100, Messina, Italy
[c] Department of Radiology, Molecular Imaging and Therapy Service, 1275 York Ave, New York, NY 10065,USA
[d] Department of Radiology, Breast Imaging Service, Memorial Sloan Kettering Cancer Center, 300 E 66th Street, New York, NY, 10065, USA

ARTICLE INFO

*Keywords:*
BRCA1 Protein
BRCA2 Protein
Breast Neoplasms
Mammography
Magnetic resonance imaging

ABSTRACT

*Objective:* To assess imaging phenotypes of familial breast cancer on mammography (MG), ultrasound (US), and magnetic resonance imaging (MRI) using the fifth edition of the BI-RADS; to investigate inter-observer agreement and to correlate imaging phenotypes with risk status, histopathology, and molecular subtypes derived by immunohistochemical surrogate.

*Materials and Methods:* Forty-nine women (BRCA-1/2 mutation carriers and women with > 20% lifetime risk) were diagnosed with breast cancer within our high-risk screening program. BI-RADS MG, US, and MRI imaging descriptors were correlated with risk status, histopathology, and molecular subtypes derived by immunohistochemical surrogate. Inter-rater agreement for BI-RADS MG, US, and MRI categories was assessed.

*Results:* Fifty-two breast cancers were diagnosed and 98% were detectable in at least one modality. MRI detected more cancers ($P < 0.001$). No lesion had benign morphology on BI-RADS. BRCA-1 had triple-negative and high-grade tumors in the posterior part and in the upper-outer quadrant ($P \leq 0.01$); positive-family-history patients had intermediate-grade neoplasms ($P < 0.01$) in the middle part ($P = 0.04$) and in the upper-outer quadrants ($P = 0.05$). There was moderate inter-rater agreement for the assigned BI-RADS assessment for MG ($k = 0.554$) and MRI ($k = 0.512$) and substantial inter-rater agreement for US ($k = 0.741$).

*Conclusions:* Imaging phenotypes of familial breast cancers with BI-RADS are malignant in all imaging modalities. Risk status seems to influence cancer location.

## 1. INTRODUCTION

Although the majority of breast cancers (BC) develop spontaneously, up to 20% of BCs occur in women with a genetic predisposition [1,2]. To achieve a significant risk reduction, these women are offered intensified annual screening or may opt for prophylactic bilateral mastectomy [3].

Based on the latest evidence, international societies have issued guidelines for high-risk BC screening, recommending magnetic resonance imaging (MRI) of the breast as a supplemental diagnostic tool [4–6]. Although MRI has the highest sensitivity in cancer detection, several investigators have stressed that high-risk BCs may show benign imaging phenotypes, potentially leading to under-diagnosis [7–13]. The Breast Imaging Reporting And Data System (BI-RADS) lexicon aims to

*Abbreviations:* MG, Mammography; US, Ultrasound; MRI, Magnetic Resonance Imaging; BI-RADS, Breast Imaging Reporting and Data System; BC, Breast Cancer; BRCA, Breast CAncer Antigen; CC, Cranio-Caudal; MLO, Medio-Lateral-Oblique; TNBC, Triple-Negative Breast Cancer; DCIS, Ductal Carcinoma In Situ; BPE, Background Parenchymal Enhancement; FGT, Fibro-Glandular Tissue; NME, Non-Mass Enhancement

* Corresponding author at: Department of Biomedical Imaging and Image-guided Therapy, Division of Molecular and Gender Imaging, Medical University of Vienna, Vienna General Hospital, Waehringer Guertel 18-20, 1090, Vienna, Austria.

*E-mail addresses:* mariaadele.marino@gmail.com (M.A. Marino), riedlc@mskcc.org (C.C. Riedl), maria.bernathova@meduniwien.ac.at (M. Bernathova), clemensbernhart@hotmail.com (C. Bernhart), pascal.baltzer@meduniwien.ac.at (P. A.T Baltzer), thomas.helbich@meduniwien.ac.at (T.H. Helbich), katja.pinker-domenig@meduniwien.ac.at (K. Pinker).

https://doi.org/10.1016/j.ejrad.2018.07.026
Received 25 April 2018; Received in revised form 21 July 2018; Accepted 28 July 2018
0720-048X/ © 2018 Elsevier B.V. All rights reserved.

provide guidance for the interpretation of breast imaging modalities [14]. The BI-RADS lexicon is being continuously updated to incorporate the inputs for cancers detection and diagnosis from original research. The 5th BI-RADS lexicon clarifies uncertain terminology for interpreting and reporting over the three imaging modalities—MG, US, and MRI [15,16].

To the best of our knowledge, this is the first study evaluating the imaging features of breast cancer in a population of high risk patients adopting the 5th BI-RADS lexicon over the three imaging modalities.

We aimed to describe imaging phenotypes in women at high-risk for BC using the 5th BI-RADS lexicon for MG, US, and MRI, to investigate the inter-observer agreement, and to correlate imaging phenotypes with mutational/risk status, histopathology, and molecular subtypes derived by immunohistochemical surrogate.

## 2. MATERIALS AND METHODS

### 2.1. Study Population

The ethics committee of our university approved this single-center study and retrospective data analysis. All participants gave written, informed consent. Participants included either tested positive for BRCA-1/2 or had a lifetime risk > 20% for the development of breast cancer. Between 01/1999-11/2015, 1365 patients (mean age 44, range: 22-83) completed 3.023 screening rounds within our institutional screening program, consisting of annual MG, US, and MRI [17]. In Austria, women are considered high-risk if their family history is positive for the following: a) three breast cancers at age ≤ 60 years; b) two breast cancers at age ≤ 50 years; c) one breast cancer at age ≤ 35 years; d) one breast cancer at age ≤ 50 years and one ovarian cancer at any age; e) two ovarian cancers at any age; and f) one male and one female cancer at any age. All the affected first-degree relatives should be on the same side of the family. The women who fulfill these criteria were advised to undergo genetic testing at our institution, but remained within the study, even if they decided not to be tested or if they tested negative for a predisposing mutation. Screening rounds consisted of mammography, ultrasound, and MRI of the breast every 12 months, with a maximum interval of one month between the individual modalities. Incomplete annual imaging rounds (i.e., one or more of the three imaging modalities were not performed) were excluded from analysis. In addition to the annual triple-modality screening rounds, ultrasound examinations were offered every six months to BRCA mutation carriers. Interval cancers were defined as cancers detected within 12 months after a screening round that was negative for malignancy. The interval cancer rate was calculated as the ratio between the number of interval cancers and the number of complete screening rounds with a follow-up of at least one year. The details of the study protocol have been described elsewhere [2]. Fifty women were diagnosed with 53 BC. One patient was excluded because the BC was detected at histopathological work-up after prophylactic mastectomy, and no imaging correlates were found. The final cohort consisted of 49 women (mean age 49, range: 27-80) diagnosed with 52 BCs (Fig. 1).

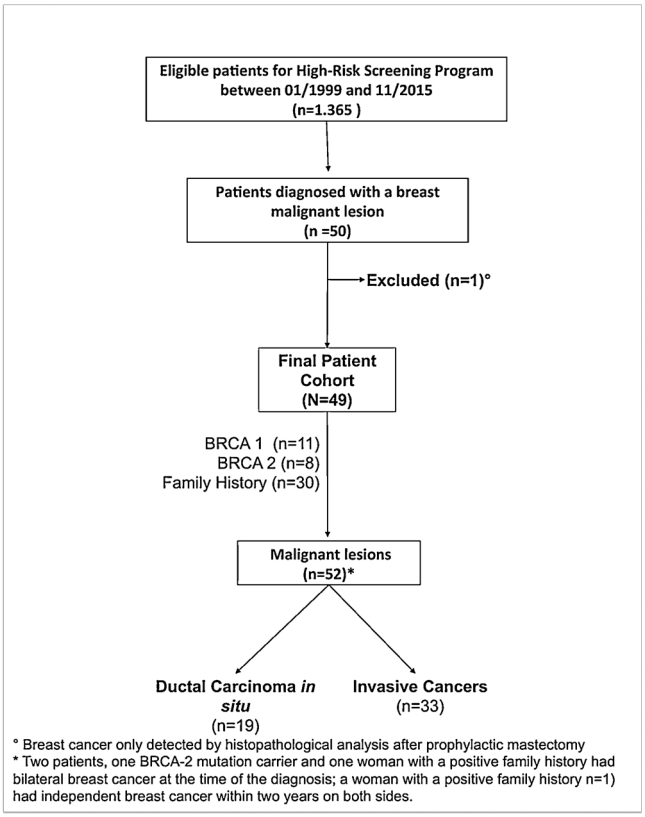


**Fig. 1.** Flowchart of study enrollment and final lesion diagnosis.

### 2.2. Imaging techniques

MG, US, and MRI have been described previously [2] and are provided in Appendix 1.

### 2.3. Data Analysis

For each BC, two breast radiologists (R1 > 15 years, R2 > 3 years of experience), blinded to the initial BI-RADS assessment but aware of final histological diagnosis of BC, independently assessed imaging features using the 5th edition BI-RADS descriptors [14] and assigned a final BI-RADS score for each modality. The readers first assessed MG images blinded to US and MRI and then, in the same session, interpreted US and MRI images. In case of discordant classifications, a consensus read was performed and a new BI-RADS classification was assigned. This was obtained in in 16/52 (30%) of cases in MG, in 8/52 (15%) for US and in 8/52 (15%) for MRI. Readers evaluated the location depth along the long axis (anterior, middle, or posterior), quadrant (upper-outer, lower-outer, medial-upper, medial-lower, and central), and side (right versus left) of lesions within the breast. Imaging features were correlated with mutation/risk status, histology, and molecular subtypes derived by immunohistochemical surrogate. Final histopathologic diagnosis was used as the reference standard. For each BC, tumor-grading and molecular subtypes, based on immunohistochemical surrogates, were assessed—luminal A (ER + and/or PR+,HER2-), luminal B (ER+ and/or PR+,HER2+), HER2-positive (ER-,PR-,HER2+), and triple-negative (TNBC) (ER-,PR-,HER2-) were recorded [18–20]. Details about the imaging features assessed according to the 5th BI-RADS lexicon for modality are provided in Tables 2, 3, and Figure 4.

### 2.4. Statistical Analysis

Statistical analyses were performed using SPSS 22.0 (SPSS,IBM,USA). Cross-tabulations were used to calculate percentages of imaging features with MG, US, and MRI. Associations of risk groups, imaging findings, and histologic results were analyzed using the Chi-square test or Fisher's exact test in case of observed numbers equal to or below 5. Differences in cancer location and risk sub-groups were tested by Fisher´s exact test. P-values (P) < / = 0.05 were considered significant. Inter-rater agreement for assigned BI-RADS categories for MG, US, and MRI, as well as the corresponding imaging features, was assessed using kappa statistics.

**Table 1**
Histologic Characteristics of Breast Cancers

| BREAST MALIGNANCY | | BRCA-1 11/52 (21%) | BRCA-2 9/52 (17%) | Family History 32/52 (61%) | TOTAL 52/52 (100%) |
|---|---|---|---|---|---|
| DUCTAL CARCINOMA IN SITU | | 2/11 (19%) | 5/9 (56%) | 12/32 (37%) | 19/52 (37%) |
| INVASIVE CARCINOMA | | 9/11 (81%) | 4/9 (44%) | 19/31 (60%) | 31/52 (60%) |
| DUCTAL NOS | | 6/9 (66%) | 3/4 (75%) | 16/19 (85%) | 25/31 (81%) |
| MEDULLARY | | 3/9 (33%) | - | - | 3/31 (10%) |
| LOBULAR | | - | - | 1/19 (5%) | 1/31 (3%) |
| MUCINOUS | | - | - | 1/19 (5%) | 1/31 (3%) |
| MICROPAPILLARY | | - | 1/4 (25%) | - | 1/31 (3%) |
| METASTASIS | | - | - | 1/32 (3%) | 1/52 (3%) |
| GRADING | | | | | **51/51 (100%)** |
| DUCTAL CARCINOMA IN SITU | GRADE 1 | - | - | 4/12 (33%) | 4/19 (21%) |
| | GRADE 2 | 1/2 (50%) | 2/5 (40%) | 4/12 (33%) | 7/19 (37%) |
| | GRADE 3 | 1/2(50%)° | 3/5 (60%) | 4/12 (33%) | 8/19 (42%) |
| INVASIVE CARCINOMA | GRADE 1 | - | - | 3/19 (16%) | 3/32 (9%) |
| | GRADE 2 | 1/9 (11%) | 2/4 (50%) | 13/19 (68%)° | 16/32 (50%) |
| | GRADE 3 | 8/9 (88%)* | 2/4 (50%) | 3/19 (16%) | 13/32 (41%) |
| RECEPTOR STATUS | | | | | **32/32(100%)** |
| INVASIVE CARCINOMA | LUMINAL A | - | 4/4 (100%) | 13/19 (67.5%) | 17/32 (55%) |
| | LUMINAL B | - | - | 2/19 (10.5%) | 2/32 (5%) |
| | TRIPLE NEG | 9/9 (100%)+ | - | 2/19 (10.5%) | 11/32 (35%) |
| | HER2/neu + | - | - | 2/19 (10.5%) | 2/32 (5%) |
| SIZE[b] | | | | | **16 ± 13 mm (3-65 mm)** |
| DUCTAL CARCINOMA IN SITU | | 4,5 ± 0,7 mm | 12,2 ± 11 mm | 14,7 ± 9 mm | 12 mm (3-35 mm) |
| INVASIVE CARCINOMA | | 23,9 ± 16,4mm | 18,2 ± 16,8 mm | 16,5 ± 14,9mm | 18 mm (3-65 mm) |
| METASTASIS | | - | - | 8 mm | 8 mm |

* P = 0.012.
\+ P = 0.000003.
° P = 0.021.
[b] Mean lesion size ± standard deviation are reported.

## 3. RESULTS

### 3.1. Patients and cancer characteristics

The tumor characteristics per subgroup of 52 cancers in 49 patients (11/49 BRCA-1, 8/49 BRCA-2 and 30/49 positive family history) are listed in Table 1. There were 19/52 (37%) ductal carcinomas in situ (DCIS), 32/52 (60%) invasive cancers, and 1/52 (3%) metastasis from ovarian cancer in a positive family history patient, which, in Table 1, is included among the invasive cancers. Mean lesion size was 12 mm (range 3-35 mm) for DCIS and 18 mm (range 3-65 mm) for invasive BC. The metastasis measured 8 mm. Among the invasive carcinomas, the most common molecular subtypes derived by immunohistochemical surrogate was luminal A (53%; 17/32; P = 0.53). In BRCA-1 mutation carriers, invasive cancers were exclusively TNBC (100%, 9/9 P < 0.01). BRCA-1 mutation carriers presented mainly with high-grade tumors (G3) for both DCIS (18% 2/11;P > 0.5) and invasive carcinomas (81%, 9/11;P = 0.012). BRCA-2 mutation carriers presented more frequently with DCIS (5/9; 56%;P > 0.5). Patients with a positive family history were associated with intermediate-grade cancers (53%, 17/32;P = 0.021).

The BI-RADS category for the three modalities and risk-groups are summarized in Appendix 2.

### 3.2. Imaging Findings for Techniques

#### 3.2.1. Mammography

Details about the imaging features on MG for all carcinomas and for each high-risk group are presented in Table 2. MG had a sensitivity of 40% (21/52) for BC detection. All cancers detected with MG showed malignant features.

Breast density patterns were analyzed for each patient, and there were no differences among the three groups (P > 0.5), or between false-negative and true-positive mammograms.

#### 3.2.2. Ultrasound

Details about the imaging features on US for all carcinomas and for each high-risk group are presented in Table 3. The sensitivity of BC detection for US was 50% (26/52). All lesions detected with US showed malignant features.

#### 3.2.3. Magnetic Resonance Imaging

Imaging features on MRI for all carcinomas and for each high-risk group are presented in Table 4. MRI detected more cancers than any other single imaging technique (MG or US) or their combination (P < 0.0001). MRI had a sensitivity of 98% (51/52) and detected 97% (32/33) of invasive cancers and 100% (19/19) of DCIS. Invasive cancers were associated with masses in 72% (37/51) (P = 0.002) and with non-mass enhancement (NME) in 14/51 (28%) (P = 0.001). Ductal carcinomas in situ were associated with NME in 58% (11/19) and with masses in 42% (8/19) of cases.

No differences were found across the three risk-groups with respect to background parenchymal enhancement (BPE) and amount of fibroglandular tissue (FGT) (P > 0.5).

### 3.3. Risk category

Details about the histopathologic diagnosis and imaging features of cancers on all imaging modalities and risk categories are presented in Tables 1–4. None of the imaging-detected cancers showed exclusively benign imaging features across the risk categories.

#### 3.3.1. BRCA-1

On MRI, 100% (11/11) of cancers with the BRCA-1 mutation were detected, which was more often than with MG, 60% (6/11), or US, 60% (6/11), P = 0.022. On MG, the majority (5/6; 83%) presented as

**Table 2**
Mammographic features stratified by histopathologic tumor type and by risk category

| MAMMOGRAPHY | | Invasive Cancer | DCIS | BRCA-1 | BRCA-2 | Family History | TOTAL |
|---|---|---|---|---|---|---|---|
| BREAST COMPOSITION (ACR BI-RADS) | | | | | | | |
| a-b | | | | 6/11 (60%) | 3/8 (37%) | 19/30 (63%) | 28/49 (58%) |
| c-d | | | | 5/11 (40%) | 5/8(63%) | 11/30 (37%) | 21/49 (42%) |
| MASSES | | | | | | | **9/21 (43%)** |
| *SHAPE* | OVAL | 0 | - | 0 | 0 | 0 | 0 |
| | ROUND | 0 | - | 0 | 0 | 0 | 0 |
| | IRREGULAR | 9/9(100%) | - | 5/5(100%) | 1/1(100%) | 3/3 (100%) | 9/9(100%) |
| *MARGINS* | CIRCUMSCRIBED | 0 | - | 0 | 0 | 0 | 0 |
| | MICROLOBULATED | 1/9 (11%) | - | 1/5 (20%) | 0 | 0 | 1/9 (11%) |
| | INDISTINCT | 3/9 (33%) | - | 2/5 (40%) | 0 | 1/3 (33%) | 3/9 (33%) |
| | SPICULATED | 5/9 (56%) | - | 2/5 (40%) | 1/1(100%) | 2/3 (67%) | 5/9 (56%) |
| *DENSITY* | HIGH | 4/9 (44%) | - | 3/5 (60%) | 0 | 1/3 (33%) | 4/9 (44%) |
| | ISODENSE | 5/9 (66%) | - | 2/5 (40%) | 1/1(100%) | 2/3 (67%) | 5/9 (66%) |
| | LOW | 0 | - | 0 | 0 | 0 | 0 |
| TOTAL | | **9/15(60%)** | **0/6 (0%)** | **5/6 (83%)** | **1/5 (20%)** | **3/10 (30%)** | |
| CALCIFICATIONS | | | | | | | **9/21 (43%)** |
| *MORPHOLOGY* | AMORPHOUS | 0 | 1/6 (17%) | 0 | 1/3 (33%) | 0 | 1/9 (11%) |
| | FINE PLEOM.[a] | 3/3 (100%) | 5/6 (83%) | 1/1(100%) | 2/3(67%) | 5/5(100%) | 8/9(89%) |
| *DISTRIBUTION* | DIFFUSE | 0 | 0 | 0 | 0 | 0 | 0 |
| | REGIONAL | 0 | 0 | 0 | 0 | 0 | 0 |
| | GROUPED | 2/3 (67%) | 3/6 (50%) | 0 | 1/3 (33%) | 4/5 (80%) | 5/9 (56%) |
| | LINEAR | 0 | 2/6 (33%) | 1/1(100%) | | 1/5 (20%) | 2/9 (22%) |
| | SEGMENTAL | 1/3 (33%) | 1/6 (17%) | 0 | 2/3 (67%) | 0 | 2/9 (22%) |
| TOTAL | | **3/15 (20%)** | **6/6 (100%)** | **1/6 (17%)** | **3/5 (60%)** | **5/10(50%)** | |
| MASS + CALCIFICATIONS | | **1/15 (7%)** | **0** | **0** | - | **1/10(10%)** | **1/21(5%)** |
| ASYMMETRIES | | **2/15 (13%)** | **0** | **0** | **1/5 (20%)** | **1/10(10%)** | **2/21(9%)** |

[a] fine pleomorphic.

masses (Fig. 2). Only one tumor (1/6; 17%) showed microcalcifications. On US, all detected cancers had malignant imaging features. On MRI, the majority (9/11; 87%) presented as masses, whereas 13% (2/11) were NME (Fig. 2).

*3.3.2. BRCA-2*

On MRI, all cancers (100%, 9/9) were detected, which was significantly more often than with MG, 56% (5/9, P = 0.029), or US, 44% (4/9, P = 0.010) (Fig. 3). Compared to the other high-risk groups, cancers in the BRCA-2 group presented more often with microcalcifications (3/5; 60%, P = 0.3). On US, 44% (4/9) of the cancers had

**Table 3**
Sonographic features stratified by histopathologic tumor type and by risk category

| ULTRASOUND | | Invasive Cancer | DCIS | BRCA-1 | BRCA-2 | Family History | TOTAL |
|---|---|---|---|---|---|---|---|
| BI-RADS DESCRIPTORS | | | | | | | |
| *SHAPE* | OVAL | 4/20 (20%) | 0 | 3/6 (50%) | 0 | 1/16 (6%) | 4/26 (16%) |
| | ROUND | 1/20 (5%) | 0 | 0 | 0 | 1/16 (6%) | 1/26 (4%) |
| | IRREGULAR | 15/20 (75%) | 6/6(100%) | 3/6 (50%) | 4/4(100%) | 14/16 (88%) | 21/26(80%) |
| *ORIENTATION* | PARALLEL | 7/20 (35%) | 2/6 (40%) | 3/6 (50%) | 2/4 (50%) | 4/16(25%) | 9/26 (35%) |
| | NOT PARALLEL | 13/20 (65%) | 4/6 (60%) | 3/6 (50%) | 2/4 (50%) | 12/16(75%) | 17/26(65%) |
| *MARGINS* | CIRCUMSCRIBED | 0 | 0 | 0 | 0 | 0 | 0 |
| | INDISTINCT | 9/20 (45%) | 3/6 (50%) | 1/6 (17%) | 2/4 (50%) | 9/16 (56%) | 12/26(46%) |
| | ANGULAR | 1/20 (5%) | 1/6 (17%) | 2/6 (33%) | 0 | 0 | 2/26 (8%) |
| | MICROLOB. | 4/20 (20%) | 2/6 (33%) | 2/6 (33%) | 1/4 (25%) | 3/16 (19%) | 6/26 (23%) |
| | SPICULATED | 6/20 (35%) | - | 1/6 (17%) | 1/4 (25%) | 4/16 (25%) | 6/26(23%) |
| *ECHO PATTERN* | ANECHOIC | 0 | 1/6 (17%) | 1/6 (17%) | 0 | 0 | 1/26 (4%) |
| | HYPERECHOIC | 1/20 (5%) | 0 | 0 | 1/4 (25%) | 0 | 1/26 (4%) |
| | COMPLEX | 0 | 1/6 (17%) | 0 | 0 | 1/16 (7%) | 1/26 (4%) |
| | HYPOECHOIC | 18/20 (90%) | 4/6 (66%) | 5/6 (83%) | 3/4 (75%) | 14/16 (86%) | 22/26(84%) |
| | ISOECHOIC | 1/20 (5%) | 0 | 0 | 0 | 1/16 (7%) | 1/26 (4%) |
| *POSTERIOR FEATURES* | NONE | 15/20 (75%) | 4/6 (66%) | 5/6 (83%) | 2/4 (50%) | 12/16 (75%) | 19/26(73%) |
| | ENHANCEMENT | 1/20 (5%) | 0 | 1/6 (17%) | 0 | 0 | 1/26 (4%) |
| | SHADOWING | 4/20 (20%) | 1/6 (17%) | 0 | 1/4 (25%) | 4/16 (22%) | 5/26 (19%) |
| | COMBINED PATTERN | 0 | 1/6 (17%) | 0 | 1/4 (25%) | 0 | 1/26 (4%) |
| *CALCIFICATIONS* | NONE | 19/20 (95%) | 5/6 (83%) | 6/6(100%) | 4/4(100%) | 14/16 (88%) | 24/26(92%) |
| | OUTSIDE A MASS | 1/20 (5%) | 0 | 0 | 0 | 1/16 (6%) | 1/26 (4%) |
| | INTRADUCTAL | 0 | 1/6 (17%) | 0 | 0 | 1/16 (6%) | 1/26 (4%) |
| *ASSOCIATED FEATURES* | NONE | 16/20 (80%) | 5/6 (83%) | 5/6 (83%) | 2/4 (50%) | 14/16 (86%) | 21/26(81%) |
| | ARCHITECTURAL DISTORTION | 3/20 (15%) | 1/6 (17%) | 1/6 (17%) | 1/4 (25%) | 2/16 (14%) | 4/26(15%) |
| | EDEMA | 1/20 (5%) | 0 | 0 | 1 (25%) | 0 | 1/26(4%) |
| *VASCULARIZATION* | NOT ASSESSED | 17/20 (85%) | 5/6(83%) | 6/6(100%) | 2/4 (50%) | 14/16(87%) | 22/26 (84%) |
| | INTERNAL | 1/20 (5%) | 1/6(17%) | 0 | 2/4 (50%) | 0 | 2/26(8%) |
| | VESSEL IN RIM | 2/20 (10%) | 0 | 0 | 0 | 2/16(13%) | 2/26 (8%) |

**Table 4**
Imaging features on MRI of the breast stratified by histopathologic tumor type and by risk category

| MAGNETIC RESONANCE IMAGING | | Invasive Cancer | DCIS | BRCA-1 | BRCA-2 | Family History | TOTAL |
|---|---|---|---|---|---|---|---|
| FIBROGLANDULAR TISSUE (FGT) | | | | | | | |
| a-b | | | | 5 (45%) | 4 (45%) | 20 (65%) | 30/52 (58%) |
| c-d | | | | 6 (55%) | 5 (55%) | 11 (35%) | 22/52 (42%) |
| BACKGROUND PARENCHYMAL ENHANCEMENT (BPE) | | | | | | | |
| MINIMAL | | | | 7 (64%) | 5 (56%) | 19 (59%) | 31/52 (60%) |
| MILD | | | | 4 (36%) | 3 (33%) | 6 (19%) | 13/52 (25%) |
| MODERATE | | | | - | - | 4 (12%) | 4/52 (7.5%) |
| MARKED | | | | - | 1 (11%) | 3 (10%) | 4/52 (7.5%) |
| MASS | | | | | | | **37/51(72%)** |
| *SHAPE* | OVAL | 3/29 (11%) | 2/8 (25%) | 1/9 (11%) | 0 | 4/22 (18%) | 5/37 (14%) |
| | ROUND | 2/29 (7%) | 1/8 (12%) | 1/9 (11%) | 0 | 2/22 (9%) | 3/37 (8%) |
| | IRREGULAR | 24/29(82%) | 5/8(63%) | 7/9 (78%) | 6/6 (100%) | 16/22(72%) | 29/37(78%) |
| *MARGINS* | CIRCUMSCRIBED | 2/29 (7%) | 2/8 (25%) | 0 | 1/6 (16%) | 3/22 (14%) | 4/37 (11%) |
| | IRREGULAR | 18/29 (62%) | 6/8 (75%) | 4/9 (44%) | 4/6 (66%) | 16/22(72%) | 24/37(64%) |
| | SPICULATED | 9/29 (31%) | 0 | 5/9 (56%) | 1/6 (16%) | 3/22 (14%) | 9/37 (25%) |
| *INTERNAL ENHANCEMENT* | HOMOGENEOUS | 11/29 (38%) | 2/8 (25%) | 2/9(22%) | 2/6 (33%) | 9/22 (41%) | 13/37(35%) |
| | HETEROGENEOUS | 11/29(38%) | 4/8 (50%) | 4/9(44%) | 1/6 (17%) | 10/22(46%) | 15/37(41%) |
| | RIM -ENHANCEMENT | 7/29 (24%) | 2/8 (25%) | 3/9(33%) | 3/6 (50%) | 3/22 (14%) | 9/37 (24%) |
| *ENHANCEMENT INITIAL PHASE* | SLOW | 1/29 (4%) | 2/8 (25%) | 1/9 (11%) | 2/6 (33%) | 0 | 3/37 (8%) |
| | MEDIUM | 4/29 (14%) | 1/8 (12%) | 2/9 (22%) | 0 | 3/22 (14%) | 5/37 (14%) |
| | FAST | 24/29(82%) | 5/8 (63%) | 6/9 (67%) | 4/6 (67%) | 19/22 (86%) | 29/37(78%) |
| *ENHANCEMENT DELAYED PHASE* | PERSISTENT | 4/29 (14%) | 2/8 (25%) | 2/9 (22%) | 1/6 (17%) | 3/21 (14%) | 6/37(16%) |
| | PLATEAU | 8/29 (28%) | 2/8 (25%) | 2/9 (22%) | 0 | 8/21 (38%) | 10/37(27%) |
| | WASH-OUT | 17/29 (58%) | 4/8 (50%) | 5/9 (56%) | 5/6 (83%) | 10/21 (47%) | 21/37(57%) |
| *TOTAL* | | 29/32 (90%) | 8/19 (42%) | 9/11 (82%) | 6/9(67%) | 22/31(71%) | - |
| NON-MASS ENHANCEMENT | | | | | | | 14/51 (28%) |
| *DISTRIBUTION* | FOCAL | 1/3 (33%) | 2/11(18%) | 0 | 2 (67%) | 1/9 (11%) | 3/14 (21%) |
| | LINEAR | 0 | 5/11 (46%) | 0 | 0 | 5/9 (56%) | 5/14 (36%) |
| | SEGMENTAL | 2/3 (67%) | 3/11 (27%) | 2/2 (100%) | 1 (33%) | 2/9 (22%) | 5/14 (36%) |
| | REGIONAL | 0 | 1/11 (9%) | 0 | 0 | 1/9 (11%) | 1/14 (7%) |
| *ENHANCEMENT INITIAL PHASE* | SLOW | 1/3 (33.3%) | 7/11 (64%) | 1/2 (50%) | 3/3 (100%) | 4/9 (45%) | 8/14 (57%) |
| | MEDIUM | 1/3 (33.3%) | 2/11 (18%) | 0 | 0 | 3/9 (33%) | 3/14 (21%) |
| | FAST | 1/3 (33.3%) | 2/11 (18%) | 1/2 (50%) | 0 | 2/9 (22%) | 3/14 (21%) |
| *ENHANCEMENT DELAYED PHASE* | PERSISTENT | 1/3 (33%) | 6/11 (55%) | 1/2 (50%) | 2 (67%) | 4/9 (45%) | 7/14 (50%) |
| | PLATEAU | 2/3 (67%) | 3/11 (27%) | 1/2 (50%) | 1 (33%) | 3/9 (33%) | 5/14 (36%) |
| | WASH-OUT | 0 | 2/11 (18%) | 0 | 0 | 2/9 (22%) | 2/14 (14%) |
| TOTAL | | **3/32 (9%)** | **11/19(58%)** | **2/11 (13%)** | **3/9 (33%)** | **9/31 (28%)** | - |

malignant imaging features. On MRI, the majority of lesions presented as masses. NME were seen in 33% (3/9) of the cases (P = 0.4).

#### 3.3.3. Positive family history for BC

On MRI, 31/32 (96%) cancers were detected significantly more often than with MG, 42% (10/32), or US, 50% (16/32), P < 0.0001. On MG, 3/10 (33.3%) had an irregular shape (100%, 3/3) with indistinct (33%, 1/3) or spiculated margins (67%, 2/3). On MG, 50% (5/10) of cancers appeared as micro-calcifications, all fine pleomorphic. On US, all cancers had malignant features. On MRI, mass lesions were seen in 70% (21/31) and NME in 30% (9/31) (Fig. 4).

### 3.4. Molecular Subtypes

#### 3.4.1. Luminal BC

Among the ER-positive invasive BCs (n = 19), 17 (89%) were luminal A, whereas two (11%) were luminal B. On MG, a total of nine (47%) lesions were detected. Of these, three (33%) lesions presented as irregularly shaped masses, with spiculated margins and characterized by a density equal to the parenchyma; three (33%) as fine pleomorphic microcalcifications; two as (22%) focal asymmetries; and one mass associated with microcalcifications (11%). On US, the majority of the lesions detected presented as irregularly shaped masses (11/13, 85%) with non-circumscribed margins (69%). Both features were significantly related to luminal A BCs (P = 0.005 and P = 0.007). On MRI, the majority of these lesions presented as irregularly shaped masses (11/17, 65%), with non-circumscribed margins (14/17, 82%), heterogeneous internal enhancement (12/17, 71%), rapid initial enhancement (13/17,76%) and washout (13/17,76%) (P > 0.001). Two lesions (12%) presented as heterogeneous and segmental NME.

#### 3.4.2. TNBC

Eleven lesions were TNBC (33%). On MG, six lesions (54 %) were detected, all presenting with irregular shape (P = 0.001), non-circumscribed margins (P = 0.002) and, isodensity (P = 0.018). On US, six (54%) lesions were detected. Two lesions had an oval shape (33%), three (50%) presented as parallel lesions, but all had non-circumscribed margins. On MRI, all TNBC were irregular-shaped masses (11/11, 100%), with non-circumscribed margins (11/11, 82%), characterized by heterogeneous (4/11, 36%) or homogeneous internal enhancement (4/11, 36%). Among the TNBCs, none presented with a slow initial enhancement. Washout (5/11, 45%) or plateau (5/11, 45%) kinetics were mainly seen in the delayed phase (P > 0.001).

#### 3.4.3. Her2-enriched

Her2-enriched BC represented 6% (2/33) of all BCs and were detectable only on MRI. These BCs presented as mass (1/2, 50%) and NME (1/2, 50%) with a heterogeneous internal enhancement pattern (2/2, 100%). In NME, the enhancement was fast at the initial phase, but persistent in the delayed phase (P > 0.001).

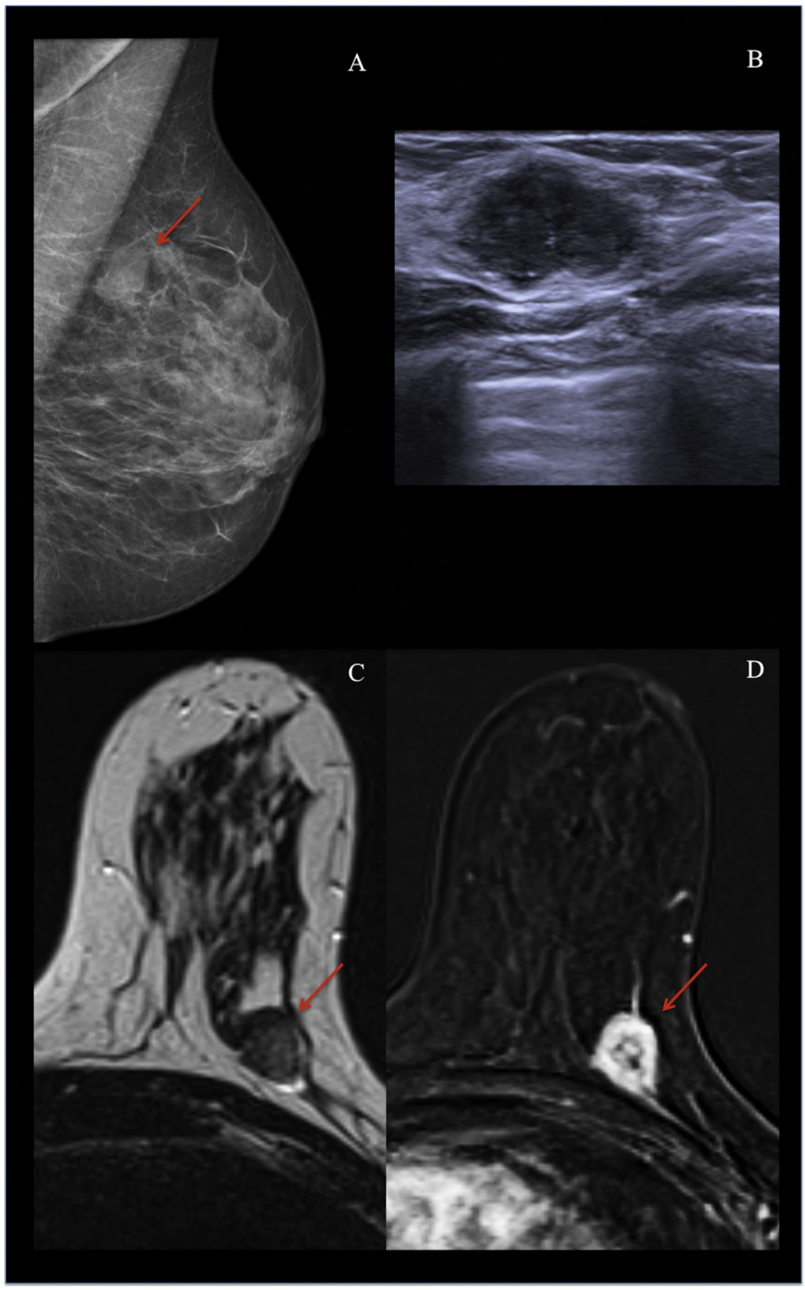


**Fig. 2.** A 36-year-old woman, a carrier of a BRCA-1 mutation, (A) Left MLO screening mammography shows scattered areas of fibroglandular density (ACR b) and demonstrates an oval mass (red arrow) with indistinct margins in the upper-outer quadrant of the left side. (B) B-mode US shows a 20 mm irregularly shaped mass and indistinct margins, with parallel orientation at 11 o´clock. (C-D) MRI of the breast (C), TSE T2w axial plane, (D) T1 FLASH 3D subtraction delayed phase (6 min). The round-shaped mass (red arrow) with irregular margins shows a rim-enhancement with a distinct vessel (feeding vessel) leading to the nodule and, in the delayed phase of the post-contrast sequences, wash-out. On T2-weighted images, the mass is hypointense surrounded by a perifocal edema. The lesion was classified as BI-RADS 5 (highly suggestive of malignancy) and biopsy was performed with final histology of invasive ductal cancer (ER- PR- Her2neu-, G3). The BRCA-1 high-risk group was also associated with a posterior location of cancers.

### *3.5. Lesion location*

Fifty-one percent (27/52) of cancers were seen in the upper-outer quadrant. This location was significantly more often seen in the BRCA-1 group (97% (10/11; P = 0.003)) than in positive family history patients (41% (13/32; P = 0.05)). Cancers in the BRCA-1 group were located significantly more often in the posterior part of the breast (73%, 8/11; P = 0.04). In positive-family-history patients, cancers were significantly more often located in the middle part of the breast (53%, 17/32; P = 0.04) (Fig. 5). Multifocal cancers were found in 19% (10/52) of the cases, independently of the risk status (P = 0.7).

### *3.6. Inter-rater agreement*

There was moderate inter-rater agreement for the assigned BI-RADS assessment for MG (k = 0.554) and MRI (k = 0.512) and substantial inter-rater agreement for US (k = 0.741). A substantial-to-almost-perfect agreement was found for the morphologic BI-RADS descriptors on MG: mass shape (k = 0.809); mass margins (k = 0.814); mass density (k = 0.957); calcification morphology (k = 0.999); and calcifications distribution (k = 0.827). Agreement for morphologic BI-RADS descriptors on US revealed substantial-to-almost-perfect agreement: mass shape (k = 0.614); mass margins (k = 0.867); mass orientation (k = 0.970); echo pattern (k = 0.837); and posterior features (k = 0.743). A moderate-to-almost-perfect agreement was found for the morphologic and functional BI-RADS descriptors on MRI: mass shape (k = 0.701); mass margins (k = 0.701); non-mass enhancement (NME) distribution (k = 0.870); internal enhancement for mass and NME (k = 0.763); kinetic curve initial phase (k = 0.673); and delayed phase (k = 0.594).

## 4. DISCUSSION

Our results indicate that imaging phenotypes of BC in high-risk women are malignant, regardless of the mutation status, the molecular status, and the imaging modality. MRI of the breast is the most sensitive

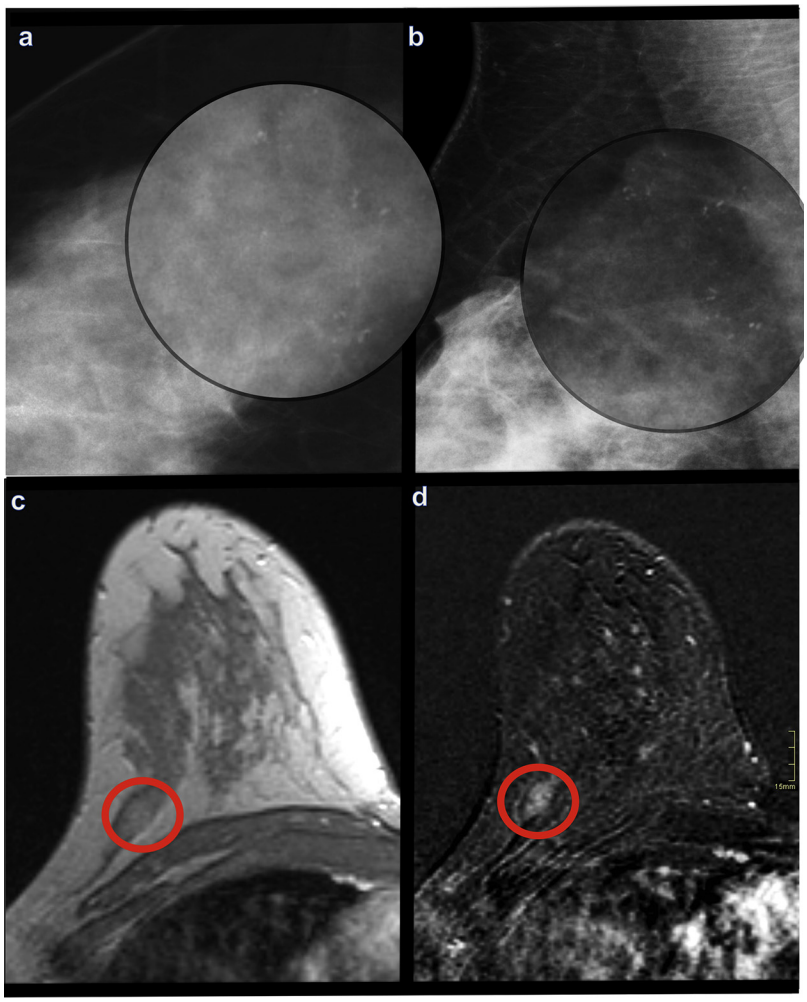


**Fig. 3.** A 46-year-old woman, a carrier of a BRCA-2 mutation, (A-B) CC (cranio-caudal) and MLO (medio-lateral-oblique) demonstrate pleomorfic microcalcifications in the upper-outer quadrant of the right breast suspicious (digital magnification, black circles). (C-D) MRI of the breast, (C) TSE T2w axial plane, (D) T1 FLASH 3D subtraction delayed phase (6 min). The irregularly shaped mass shows non-circumscribed margins and demonstrates heterogeneous enhancement with washout kinetics in the delayed phase and hypointensity on T2-weighted images. The lesion was classified as BI-RADS 5 (highly suggestive of malignancy) and a stereotactic vacuum assisted biopsy was performed of the area of the highly suspicious microcalcification, yielding a final histology of invasive ductal cancer (ER + PR+ Her2neu-, G2).

test for cancer detection. With the 5$^{th}$ BI-RADS lexicon edition, a correct classification of high-risk BCs is feasible. BRCA-2 associated carcinomas more often exhibit microcalcifications on MG compared to other risk categories associated with cancers. Tumor location seems to be influenced by the risk status.

All cancers presented at least one BI-RADS malignant imaging feature on MG, US, and MRI. Cancers visible on MG (40%) showed suspicious morphology and were classified as BI-RADS 4/5. Masses presented with an irregular shape and non-circumscribed margins, while microcalcifications were fine pleomorphic with grouped, linear, and segmental distributions (100%). Cancers detected with ultrasound (50%) presented with at least one imaging feature classified as malignant by BI-RADS. While cancers presented with varying BI-RADS descriptors for shape, orientation, echo pattern, and posterior features, a consistent finding across tumor types and risk groups was that no cancers had circumscribed margins on US. Our data indicate that margin is the most reliable BI-RADS US descriptor for an accurate diagnosis in high-risk patients. This is in good agreement with Schrading et al. [7], who also found irregular shape and margins most frequently. In contrast to published data [7,21], none of the lesions in our cohort showed purely benign features. In our study margins were non-circumscribed but they could be considered rather circumscribed when compared to the classic appearance of BCs. This fact should not be mistaken for circumscribed margins that usually refer to the pseudo-capsulated appearance of fibroadenomas and should always be assessed in post-contrast images [14,22].

BRCA-1 mutation carriers often present with higher grade and TNBC compared to non-carriers [23–30], with rates of TNBC ranging from 50%-88%. In this study, in 9/11 cases (81%) of BRCA-1 carriers the diagnosis of invasive BC was made. Eighty-eight percent were grade 3 at diagnosis and all were TNBC (100%). High-risk BCs that presented with benign imaging phenotypes [7–10] have been attributed to the frequent occurrence of TNBC, which reportedly exhibits relatively benign morphologic features, such as smooth margins and rim enhancement [7–9,30]. However, a significant number of TNBCs do not show these benign phenotypes [31–33]. In our cohort, TNBCs were related to irregular shape ($P = 0.001$) and spiculated margins ($P = 0.002$), with a density equal to the parenchyma on mammography ($P = 0.01$). On MRI, they were associated with non-circumscribed margins ($P = 0.04$), heterogeneous enhancement ($P = 0.04$), and fast initial enhancement ($P = 0.06$).

While microcalcifications are found in 40%-75% of BCs in the general female population [28,34], high-risk BCs less commonly present with microcalcifications [7,11,21]. This is confirmed in our results, where only 17% (9/52) of BCs showed microcalcifications: 3/33 (9%) invasive cancers and 6/19 (32%) DCIS. Previous findings reported that BRCA-2 patients have a higher rate of microcalcifications compared to BRCA-1 or positive-history patients, with 33% vs 9% vs 16%, respectively [11,21,35]. Schrading et al. [7] found microcalcifications in 50% of cancers in their patients with a BRCA-2 mutation. In our study, BRCA-2 carriers were also more likely to present with pure DCIS or DCIS associated with invasive cancer, confirming previous results [35].

MRI is the most sensitive test for high-risk BC (98%), regardless of risk group. MRI outperforms mammography, ultrasound and the combination of these two modalities, respectively with a sensitivity of 40% and 50% ($P < 0.0001$), with almost half of all cancers (45%) detected

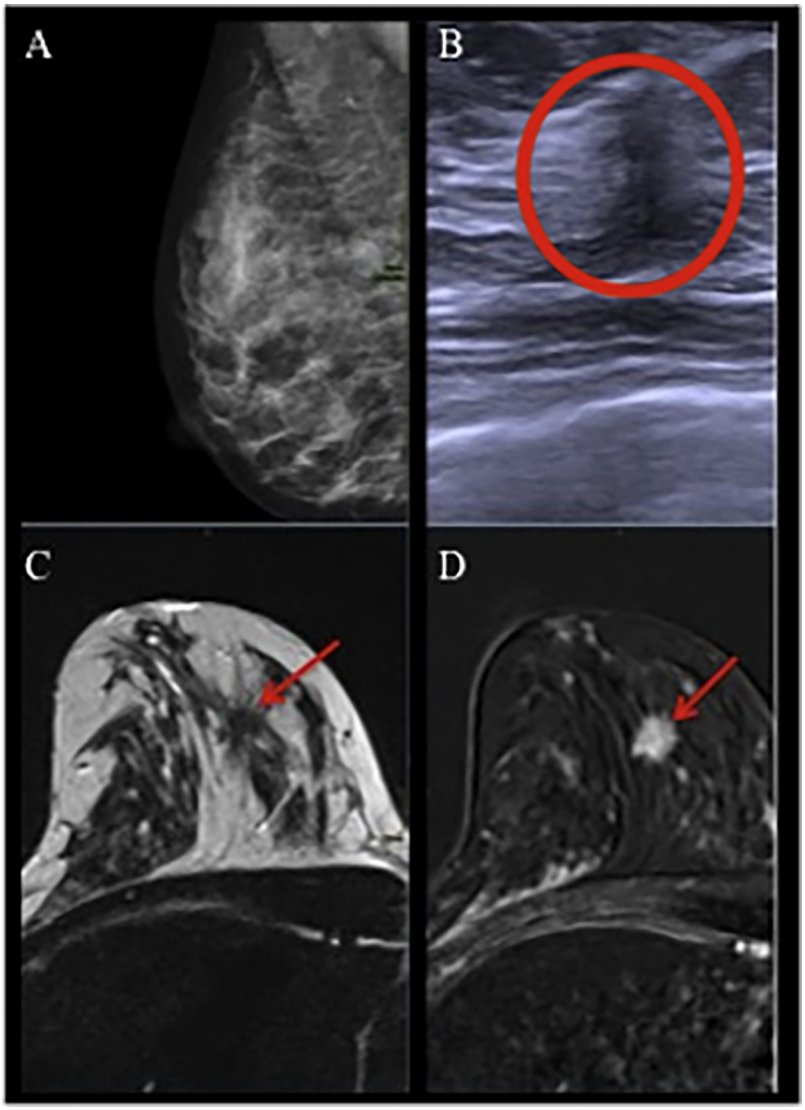


**Fig. 4.** A 41-year-old woman with a positive family history. (A) MLO (medio-lateral-oblique) of the right breast. The breast is heterogeneously dense, which could obscure a small mass (ACR c). No visible lesion on the breast, with small axillary lymph nodes, BI-RADS 1 (negative). (B) B-mode US shows a 7 mm irregularly shaped mass and indistinct margins (red circle), with a not-parallel orientation at 1 o´clock of the right breast. (C-D) MRI of the breast, (C) TSE T2w axial plane, (D) T1 FLASH 3D subtraction delayed phase (6 min). The irregularly shaped mass with spiculated margins shows heterogeneous and continuous (plateau) enhancement and hypointensity on T2-weighted images. The final BI-RADS score was reported as 5 (highly suggestive of malignancy) and the final histology yielded invasive ductal carcinoma, (ER + PR + Her2neu-) G2.

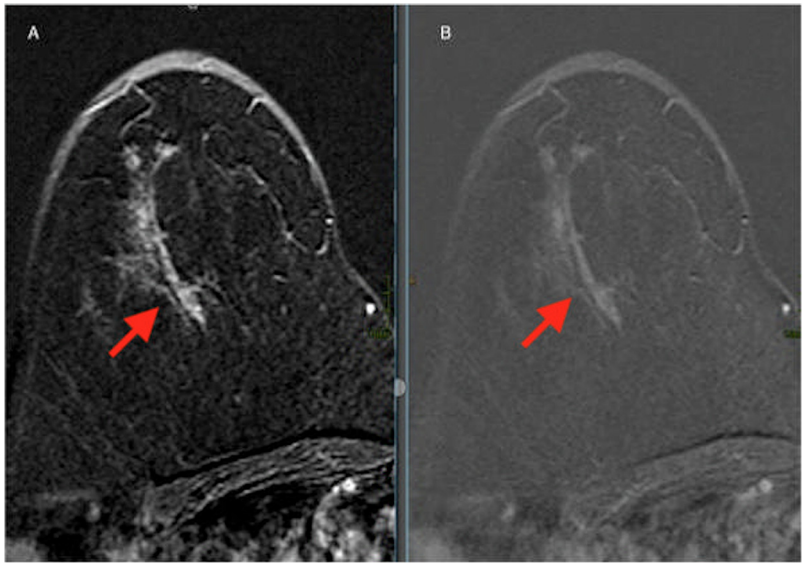


**Fig. 5.** A 40-year-old woman with a positive family history for breast cancer. The positive-family-history high-risk group was associated with cancers located in the middle part of the breast. MRI of the breast (A) DCE T1 FAT-SAT and (B) subtraction at 2 min with a linear non-mass enhancement (red arrows). The final histology revealed a ductal carcinoma in situ.

by MRI only. Schrading et al. [7] demonstrated that the specificity and positive predictive value of MRI is high. Obdeijn et al. [36] found, in a population of 93 BRCA-1 mutation-carriers, a sensitivity of 93.6% for MRI alone, with no additional value for mammography in MRI screening for women below the age of 40. Riedl et al. [2] demonstrated that MRI in high-risk patients had a sensitivity of 90% and almost half of all cancers (45%) in their cohort were detected by MRI only.

All cancers visible on MRI (98%) showed at least one suspicious feature and were, therefore, assigned final BI-RADS categories 4/5. Cancers almost exclusively exhibited malignant morphologic imaging features, with only one lesion with features (shape and margins) suggestive of benignity. Kinetic analysis of the lesion showed an initial fast/persistent enhancement with a heterogeneous internal enhancement pattern, an uncommon feature for benignity. Veltman et al. [9] and Schrading et al. [7] reported that patients with BRCA mutations exhibited benign morphologic features more frequently, yet kinetic analysis of these masses revealed malignant curves [37]. In our study, in NME, enhancement curves were commonly benign in both phases. Fifty-eight percent (11/19) of NME were DCIS, which often have weak angiogenetic activity. None of these lesions would have been correctly identified as malignant based on kinetics alone, but the combined analysis of morphologic and kinetic descriptors enabled an accurate classification. The current study adds to the growing body of evidence that MRI is superior to MG and US in high-risk patients [11,38], and thus, these other modalities may be omitted in high-risk screening.

For MG, five (36%) false-negatives occurred in BRCA-1, four (44%) in BRCA-2, and 22 (69%) in family-history patients. Only three (9%) cases occurred in patients with entirely fatty breasts and these lesions were small (< 15 mm). On US, five cases occurred in BRCA-1 (36%), five (55%) in BRCA-2, and 16 (50%) in family-history patients, which were cases of either very small lesions (5-11 mm) or DCIS.

Prior studies have shown that high-risk cancers may show a preferred location in the upper-outer quadrant of the breast: 52% in the study by Schrading et al. [7] and 27% in the study by Trecate et al. [8]. In our study, 46% (24/52) were located in the posterior part and 42% (22/52) in the middle part of the breast. In our cohort, 73% of BRCA-1 BCs were located in the posterior part of the breast (P = 0.05). This supports data from Schrading et al. [7], who showed that BRCA-1 mutation carriers tend to develop cancers in the posterior part of the breast. Our study also demonstrated that BCs occurring in patients with a positive family history present in the middle/central portion of the breast (53%, 17/32; P = 0.04). This is the first study to show a predilection of BCs in family-history patients for the middle portion of the breast, which is distinctly different from BRCA carriers and should be taken into consideration when reporting this patient population.

This study has some limitations. The sample size is small which may limit strong conclusion yet, it has to be noted that it is one of the largest ever reported in the literature that includes imaging phenotype analyses with MG, US, and MRI. During the study, imaging techniques and software were updated, yet all examinations were performed with state-of-the-art equipment and adhered to international recommendations [4,5].

In conclusion, imaging phenotypes of familial BC are malignant regardless of the mutation status, molecular subtypes derived by immunohistochemical surrogate, or the imaging modality used. The 5$^{th}$ BI-RADS lexicon edition enables a correct classification with all the imaging technologies. MRI is significantly more sensitive for the detection of high-risk BCs compared to MG and US. Radiologists should be aware of the association of different risk status groups with tumor type and location.

This research did not receive any specific grant from funding agencies in the public, commercial, or not-for-profit sectors.

## CONFLICT OF INTEREST

None

## Appendix A. Supplementary DATA

Supplementary material related to this article can be found, in the online version, at doi:https://doi.org/10.1016/j.ejrad.2018.07.026.

## References

[1] Familial breast cancer: collaborative reanalysis of individual data from 52 epidemiological studies including 58 209 women with breast cancer and 101 986 women without the disease, The Lancet. 358 (2001) 1389–1399, https://doi.org/10.1016/S0140-6736(01)06524-2.

[2] C.C. Riedl, N. Luft, C. Bernhart, M. Weber, M. Bernathova, M.-K.M. Tea, M. Rudas, C.F. Singer, T.H. Helbich, Triple-modality screening trial for familial breast cancer underlines the importance of magnetic resonance imaging and questions the role of mammography and ultrasound regardless of patient mutation status, age, and breast density, J. Clin. Oncol. 33 (2015) 1128–1135, https://doi.org/10.1200/JCO.2014.56.8626.

[3] S. van Dijk, M.S. van Roosmalen, W. Otten, P.F.M. Stalmeier, Decision making regarding prophylactic mastectomy: stability of preferences and the impact of anticipated feelings of regret, J. Clin. Oncol. 26 (2008) 2358–2363, https://doi.org/10.1200/JCO.2006.10.5494.

[4] R.M. Mann, C. Balleyguier, P.A. Baltzer, U. Bick, C. Colin, E. Cornford, A. Evans, E. Fallenberg, G. Forrai, M.H. Fuchsjäger, F.J. Gilbert, T.H. Helbich, S.H. Heywang-Köbrunner, J. Camps-Herrero, C.K. Kuhl, L. Martincich, F. Pediconi, P. Panizza, L.J. Pina, R.M. Pijnappel, K. Pinker-Domenig, P. Skaane, F. Sardanelli, European Society of Breast Imaging (EUSOBI), with language review by Europa Donna–The European Breast Cancer Coalition, Breast MRI: EUSOBI recommendations for women's information, Eur Radiol. (2015), https://doi.org/10.1007/s00330-015-3807-z.

[5] F. Sardanelli, C. Boetes, B. Borisch, T. Decker, M. Federico, F.J. Gilbert, T. Helbich, S.H. Heywang-Köbrunner, W.A. Kaiser, M.J. Kerin, R.E. Mansel, L. Marotti, L. Martincich, L. Mauriac, H. Meijers-Heijboer, R. Orecchia, P. Panizza, A. Ponti, A.D. Purushotham, P. Regitnig, M.R. Del Turco, F. Thibault, R. Wilson, Magnetic resonance imaging of the breast: Recommendations from the EUSOMA working group, European Journal of Cancer. 46 (2010) 1296–1316, https://doi.org/10.1016/j.ejca.2010.02.015.

[6] C.K. Kuhl, K. Strobel, H. Bieling, C. Leutner, H.H. Schild, S. Schrading, Supplemental Breast MR Imaging Screening of Women with Average Risk of Breast Cancer, Radiology 283 (2017) 361–370, https://doi.org/10.1148/radiol.2016161444.

[7] S. Schrading, C.K. Kuhl, Mammographic, US, and MR imaging phenotypes of familial breast cancer, Radiology 246 (2008) 58–70, https://doi.org/10.1148/radiol.2461062173.

[8] G. Trecate, R. Agresti, L. Suman, D. Vergnaghi, B. Valeri, M. Marchesini, C. Ferranti, C. Ferraris, S. Manoukian, G. Scaperrotta, S. Viganò, P. Panizza, What is specific in hereditary breast cancer? High T2 signal intensity as a new semeiotic pattern? Eur J Radiol. 81 (Suppl 1) (2012) S165–170, https://doi.org/10.1016/S0720-048X(12)70069-4.

[9] J. Veltman, R. Mann, T. Kok, I.M. Obdeijn, N. Hoogerbrugge, J.G. Blickman, C. Boetes, Breast tumor characteristics of BRCA1 and BRCA2 gene mutation carriers on MRI, European Radiology. 18 (2008) 931–938, https://doi.org/10.1007/s00330-008-0851-y.

[10] X.-A. Phi, S. Saadatmand, G.H. De Bock, E. Warner, F. Sardanelli, M.O. Leach, C.C. Riedl, I. Trop, M.J. Hooning, R. Mandel, F. Santoro, G. Kwan-Lim, T.H. Helbich, M.M. Tilanus-Linthorst, E.R. van den Heuvel, N. Houssami, Contribution of mammography to MRI screening in BRCA mutation carriers by BRCA status and age: individual patient data meta-analysis, Br. J. Cancer (2016), https://doi.org/10.1038/bjc.2016.32.

[11] F.J. Gilbert, R.M.L. Warren, G. Kwan-Lim, D.J. Thompson, R.A. Eeles, D.G. Evans, M.O. Leach, United Kingdom Magnetic Resonance Imaging in Breast Screening (MARIBS) Study Group, Cancers in BRCA1 and BRCA2 carriers and in women at high risk for breast cancer: MR imaging and mammographic features, Radiology 252 (2009) 358–368, https://doi.org/10.1148/radiol.2522081032.

[12] J.M. Noh, B.-K. Han, D.H. Choi, S.J. Rhee, E.Y. Cho, S.J. Huh, W. Park, H. Park, S.J. Nam, J.E. Lee, W.-H. Kil, Association between BRCA Mutation Status, Pathological Findings, and Magnetic Resonance Imaging Features in Patients with Breast Cancer at Risk for the Mutation, J Breast Cancer 16 (2013) 308–314, https://doi.org/10.4048/jbc.2013.16.3.308.

[13] M.V. Lee, V.S. Katabathina, M.L. Bowerson, M.I. Mityul, A.S. Shetty, K.M. Elsayes, A. Balachandran, P.R. Bhosale, A.E. McCullough, C.O. Menias, BRCA-associated Cancers: Role of Imaging in Screening, Diagnosis, and Management, Radiographics 37 (2017) 1005–1023, https://doi.org/10.1148/rg.2017160144.

[14] C.J. D'Orsi, E.A. Sickles, E.B. Mendelson, E.A. Morris, et al., ACR BI-RADS® Atlas, Breast Imaging Reporting and Data System (n.d.), American College of Radiology, Reston, VA, 2013 (Accessed 20 September 2015), http://www.acr.org/~/media/ACR/Documents/PDF/QualitySafety/Resources/BIRADS/BIRADS%20V5%20Changes.pdf.

[15] M. Benndorf, P.A.T. Baltzer, W.A. Kaiser, Assessing the degree of collinearity among the lesion features of the MRI BI-RADS lexicon, Eur J Radiol. 80 (2011) e322–324, https://doi.org/10.1016/j.ejrad.2010.11.030.

[16] P.A.T. Baltzer, M. Benndorf, M. Dietzel, M. Gajda, I.B. Runnebaum, W.A. Kaiser, False-positive findings at contrast-enhanced breast MRI: a BI-RADS descriptor study, AJR Am J Roentgenol. 194 (2010) 1658–1663, https://doi.org/10.2214/AJR.09.3486.

[17] C.F. Singer, M.-K. Tea, G. Pristauz, M. Hubalek, C. Rappaport, C. Riedl, T. Helbich, Guideline for the prevention and early detection of breast and ovarian cancer in high risk patients, particularly in women from HBOC (hereditary breast and ovarian cancer) families, Wien. Klin. Wochenschr. 124 (2012) 334–339, https://doi.org/10.1007/s00508-012-0173-6.
[18] C.M. Perou, T. Sørlie, M.B. Eisen, M. van de Rijn, S.S. Jeffrey, C.A. Rees, J.R. Pollack, D.T. Ross, H. Johnsen, L.A. Akslen, O. Fluge, A. Pergamenschikov, C. Williams, S.X. Zhu, P.E. Lønning, A.L. Børresen-Dale, P.O. Brown, D. Botstein, Molecular portraits of human breast tumours, Nature 406 (2000) 747–752, https://doi.org/10.1038/35021093.
[19] Cancer Genome Atlas Network, Comprehensive molecular portraits of human breast tumours, Nature 490 (2012) 61–70, https://doi.org/10.1038/nature11412.
[20] S.R. Lakhani, The Pathology of Familial Breast Cancer: Predictive Value of Immunohistochemical Markers Estrogen Receptor, Progesterone Receptor, HER-2, and p53 in Patients With Mutations in BRCA1 and BRCA2, Journal of Clinical Oncology. 20 (2002) 2310–2318, https://doi.org/10.1200/JCO.2002.09.023.
[21] L.J. Hamilton, A.J. Evans, A.R.M. Wilson, N. Scott, E.J. Cornford, S.E. Pinder, H.N. Khan, R.D. Macmillan, Breast imaging findings in women with BRCA1- and BRCA2-associated breast carcinoma, Clin Radiol. 59 (2004) 895–902, https://doi.org/10.1016/j.crad.2004.03.013.
[22] M.A. Marino, P. Clauser, R. Woitek, G.J. Wengert, P. Kapetas, M. Bernathova, K. Pinker-Domenig, T.H. Helbich, K. Preidler, P.A.T. Baltzer, A simple scoring system for breast MRI interpretation: does it compensate for reader experience? Eur Radiol. (2015), https://doi.org/10.1007/s00330-015-4075-7.
[23] S.R. Lakhani, The pathology of familial breast cancer: Morphological aspects, Breast Cancer Res. 1 (1999) 31–35.
[24] B.J. Lynch, J.A. Holden, S.S. Buys, S.L. Neuhausen, D.K. Gaffney, Pathobiologic characteristics of hereditary breast cancer, Hum. Pathol. 29 (1998) 1140–1144.
[25] Pathology of familial breast cancer: differences between breast cancers in carriers of BRCA1 or BRCA2 mutations and sporadic cases. Breast Cancer Linkage Consortium, Lancet 349 (1997) 1505–1510.
[26] T. Byrski, T. Huzarski, R. Dent, J. Gronwald, D. Zuziak, C. Cybulski, J. Kladny, B. Gorski, J. Lubinski, S.A. Narod, Response to neoadjuvant therapy with cisplatin in BRCA1-positive breast cancer patients, Breast Cancer Res. Treat. 115 (2009) 359–363, https://doi.org/10.1007/s10549-008-0128-9.
[27] A. Musolino, N. Naldi, M. Michiara, M.A. Bella, P. Zanelli, B. Bortesi, M. Capelletti, M. Savi, T.M. Neri, A. Ardizzoni, A breast cancer patient from Italy with germline mutations in both the BRCA1 and BRCA2 genes, Breast Cancer Res. Treat. 91 (2005) 203–205, https://doi.org/10.1007/s10549-004-7704-4.
[28] S.E. Karp, P.N. Tonin, L.R. Bégin, J.J. Martinez, J.C. Zhang, M.N. Pollak, W.D. Foulkes, Influence of BRCA1 mutations on nuclear grade and estrogen receptor status of breast carcinoma in Ashkenazi Jewish women, Cancer 80 (1997) 435–441.
[29] A. Musolino, M.A. Bella, B. Bortesi, M. Michiara, N. Naldi, P. Zanelli, M. Capelletti, D. Pezzuolo, R. Camisa, M. Savi, T.M. Neri, A. Ardizzoni, BRCA mutations, molecular markers, and clinical variables in early-onset breast cancer: a population-based study, Breast 16 (2007) 280–292, https://doi.org/10.1016/j.breast.2006.12.003.
[30] O.T. Jóhannsson, I. Idvall, C. Anderson, A. Borg, R.B. Barkardóttir, V. Egilsson, H. Olsson, Tumour biological features of BRCA1-induced breast and ovarian cancer, Eur. J. Cancer 33 (1997) 362–371.
[31] T. Uematsu, M. Kasami, S. Yuen, Triple-negative breast cancer: correlation between MR imaging and pathologic findings, Radiology 250 (2009) 638–647, https://doi.org/10.1148/radiol.2503081054.
[32] K.M. Krizmanich-Conniff, C. Paramagul, S.K. Patterson, M.A. Helvie, M.A. Roubidoux, J.D. Myles, K. Jiang, M. Sabel, Triple receptor-negative breast cancer: imaging and clinical characteristics, AJR Am J Roentgenol. 199 (2012) 458–464, https://doi.org/10.2214/AJR.10.6096.
[33] E.B. Ryu, J.M. Chang, M. Seo, S.A. Kim, J.H. Lim, W.K. Moon, Tumour volume doubling time of molecular breast cancer subtypes assessed by serial breast ultrasound, Eur Radiol. 24 (2014) 2227–2235, https://doi.org/10.1007/s00330-014-3256-0.
[34] V. Castronovo, A. Bellahcene, Evidence that breast cancer associated microcalcifications are mineralized malignant cells, Int. J. Oncol. 12 (1998) 305–308.
[35] J. Krammer, K. Pinker-Domenig, M.E. Robson, M. Gönen, B. Bernard-Davila, E.A. Morris, D.A. Mangino, M.S. Jochelson, Breast cancer detection and tumor characteristics in BRCA1 and BRCA2 mutation carriers, Breast Cancer Res. Treat. 163 (2017) 565–571, https://doi.org/10.1007/s10549-017-4198-4.
[36] I.-M. Obdeijn, G.A.O. Winter-Warnars, R.M. Mann, M.J. Hooning, M.G.M. Hunink, M.M.A. Tilanus-Linthorst, Should we screen BRCA1 mutation carriers only with MRI? A multicenter study, Breast Cancer Res. Treat. 144 (2014) 577–582, https://doi.org/10.1007/s10549-014-2888-8.
[37] C. Kuhl, The current status of breast MR imaging. Part I. Choice of technique, image interpretation, diagnostic accuracy, and transfer to clinical practice, Radiology 244 (2007) 356–378, https://doi.org/10.1148/radiol.2442051620.
[38] C.K. Kuhl, S. Schrading, S. Weigel, K. Nüssle-Kügele, H. Sittek, B. Arand, N. Morakkabati, C. Leutner, B. Tombach, D. Nordhoff, C. Perlet, A. Rieber, W. Heindel, H.J. Brambs, H. Schild, The “EVA” Trial: Evaluation of the Efficacy of Diagnostic Methods (Mammography, Ultrasound, MRI) in the secondary and tertiary prevention of familial breast cancer, Preliminary results after the first half of the study period], Rofo. 177 (2005) 818–827, https://doi.org/10.1055/s-2005-858203.